

MULTIWAVELENGTH FOLLOW-UP OF THE HYPERLUMINOUS INTERMEDIATE-MASS BLACK HOLE CANDIDATE 3XMM J215022.4–055108

DACHENG LIN¹, JAY STRADER², AARON J. ROMANOWSKY^{3,4}, JIMMY A. IRWIN⁵, OLIVIER GODET^{6,7}, DIDIER BARRET^{6,7},
NATALIE A. WEBB^{6,7}, JEROEN HOMAN^{8,9}, RONALD A. REMILLARD¹⁰

Draft version February 13, 2020

ABSTRACT

We recently discovered the X-ray/optical outbursting source 3XMM J215022.4–055108. It was best explained as the tidal disruption of a star by an intermediate-mass black hole of mass of a few tens of thousand solar masses in a massive star cluster at the outskirts of a large barred lenticular galaxy at $D_L = 247$ Mpc. However, we could not completely rule out a Galactic cooling neutron star as an alternative explanation for the source. In order to further pin down the nature of the source, we have obtained new multiwavelength observations by *XMM-Newton* and *Hubble Space Telescope (HST)*. The optical counterpart to the source in the new *HST* image is marginally resolved, which rules out the Galactic cooling neutron star explanation for the source and suggests a star cluster of half-light radius ~ 27 pc. The new *XMM-Newton* observation indicates that the luminosity was decaying as expected for a tidal disruption event and that the disk was still in the thermal state with a super-soft X-ray spectrum. Therefore, the new observations confirm the source as one of the best intermediate-mass black hole candidates.

Subject headings: accretion, accretion disks — black hole physics — X-rays: galaxies — galaxies: individual: 3XMM J215022.4-055108

1. INTRODUCTION

There has been strong evidence for the existence of stellar-mass black holes (BHs, mass $\sim 10 M_\odot$) from dynamical measurements (Remillard & McClintock 2006) and gravitational wave detections (Abbott et al. 2016). The evidence for the existence of supermassive BHs (SMBHs, mass $\sim 10^6$ – $10^{10} M_\odot$) at the centers of massive galaxies is also very compelling (Kormendy & Richstone 1995; Gillessen et al. 2009; Gravity Collaboration et al. 2018; Event Horizon Telescope Collaboration et al. 2019). However, intermediate-mass BHs of mass $\sim 10^3$ – $10^5 M_\odot$ are still observationally elusive despite the long-term search (see Greene et al. 2019, for a recent review). Some candidates were found from a variety of systems, including dwarf galaxies (e.g., Dong et al. 2007; Baldassare et al. 2015; Chilingarian et al. 2018), globular clusters (e.g., Irwin et al. 2010; Kızıltan et al. 2017; Noyola et al. 2008; Perera et al. 2017), and hyperluminous off-nuclear X-ray sources (HLXs, X-ray

luminosity $L_X \geq 10^{41}$ erg s⁻¹, Farrell et al. 2009; Webb et al. 2012; Lin et al. 2016). Confirming the IMBH nature of these candidates is non-trivial, as there is no well accepted feasible method to weigh these BHs. The inference of the IMBHs in globular clusters depends on the models/methods used to infer their presence and is typically called into question in follow-up studies (e.g., Mann et al. 2019; Baumgardt et al. 2019). HLXs are interesting IMBH candidates, but it is important to rule out background AGNs (Sutton et al. 2015) or even accreting neutron stars (Israel et al. 2017).

We reported our discovery of a new HLX candidate 3XMM J215022.4–055108 (J2150–0551 hereafter) in Lin et al. (2018, Lin18 hereafter). The source exhibited a prolonged X-ray outburst of peak X-ray flux of $\sim 10^{-12}$ erg s⁻¹ cm⁻², lasting for more than a decade and X-ray spectra soft and purely thermal. The outburst was also detected in the optical. The source is located at the outskirts of a large barred lenticular galaxy (Gal1 hereafter) at $z = 0.055$, and we identified a faint optical counterpart based on the positional coincidence and the correlated optical/X-ray variability. The most promising explanation for the source is that it is an IMBH in an off-center star cluster with the X-ray/optical outburst (peak X-ray luminosity $\sim 7 \times 10^{42}$ erg s⁻¹) due to a tidal disruption event (TDE), in which a star having a close encounter with the BH was tidally disrupted and subsequently accreted, producing the multiwavelength flare (see Komossa 2015, for a recent review). We measured the BH mass to be $\sim 5 \times 10^4 M_\odot$, based on the fit to the X-ray spectra, which we assumed to be in the thermal state during the decay. The thermal state identification was supported by the fact that the X-ray spectra can be described well with a standard thin disk, whose temperature and luminosity approximately followed the $L \propto T^4$ relation. The event was later modeled in detail

¹ Space Science Center, University of New Hampshire, Durham, NH 03824, USA, email: dacheng.lin@unh.edu

² Center for Data Intensive and Time Domain Astronomy, Department of Physics and Astronomy, Michigan State University, 567 Wilson Road, East Lansing, MI 48824, USA

³ Department of Physics and Astronomy, San José State University, One Washington Square, San José, CA 95192, USA

⁴ University of California Observatories, 1156 High Street, Santa Cruz, CA 95064, USA

⁵ Department of Physics and Astronomy, University of Alabama, Box 870324, Tuscaloosa, AL 35487, USA

⁶ CNRS, IRAP, 9 avenue du Colonel Roche, BP 44346, F-31028 Toulouse Cedex 4, France

⁷ Université de Toulouse, UPS-OMP, IRAP, Toulouse, France

⁸ Eureka Scientific, Inc., 2452 Delmer Street, Oakland, California 94602, USA

⁹ SRON, Netherlands Institute for Space Research, Sorbonnelaan 2, 3584 CA Utrecht, The Netherlands

¹⁰ MIT Kavli Institute for Astrophysics and Space Research, MIT, 70 Vassar Street, Cambridge, MA 02139-4307, USA

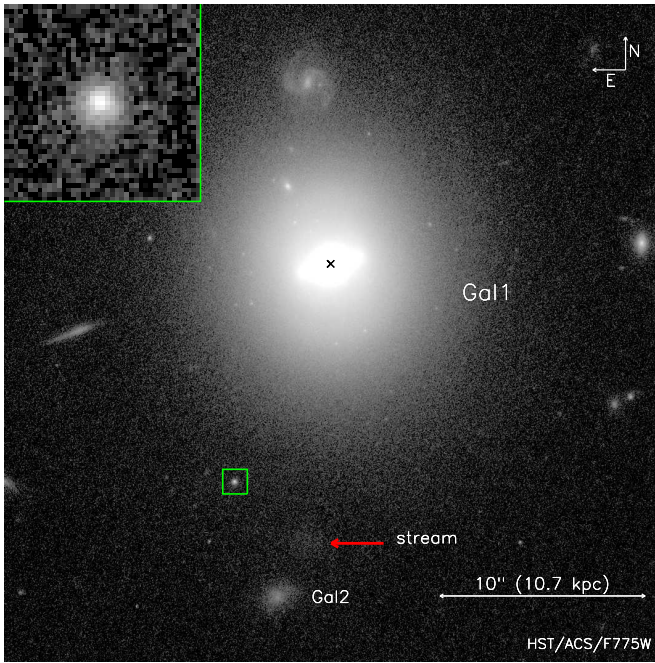


FIG. 1.— The new *HST* image around the field of J2150–0551. The green box of $1''.2 \times 1''.2$, with zoomed inset, is centered around the source and is the region that we used to carry out the profile fitting (Section 3). Gal1 is the main host galaxy of the source, and near the source is a possible satellite galaxy Gal2, which might be connected with Gal1 by a tidal stream.

by Chen & Shen (2018), who inferred a main-sequence disrupted star of mass $0.33 M_{\odot}$ and radius $0.41 R_{\odot}$.

The star cluster was not clearly resolved in a *Hubble Space Telescope* (*HST*) Advanced Camera for Surveys (ACS) Wide Field Camera (WFC) F775W image in 2003 before the outburst. This is probably due to the low signal-to-noise ratio of the source in this image, in which the source fell into the CCD gap in two of four exposures. Based on the fit to the broad-band quiescent photometry, we inferred the stellar mass of the cluster to be $\sim 10^7 M_{\odot}$, making it either a massive globular cluster or an ultra-compact dwarf (UCD) galaxy, which has physical properties intermediate between classical globular clusters and galaxies and is often explained as a remnant nucleus of a tidally stripped dwarf galaxy (Norris et al. 2014).

There is an alternative explanation for the faint X-ray outburst of the source: the cooling of the crust of a Galactic neutron star heated in a large accretion outburst. The main problem with this explanation is that the accretion outburst was not detected by the All-sky Monitor onboard *RXTE* and would therefore be too weak to heat up the crust of the neutron star (Lin18).

In order to differentiate the above two explanations, we obtained follow-up observations with *XMM-Newton* and *HST* in 2018. The *XMM-Newton* observation served to monitor the X-ray flux and spectral evolution and to check whether the luminosity continues to decrease as expected for a TDE. The *HST* image served to check whether the optical counterpart is extended or not. In this Letter we report the results of these new observations. In Section 2, we describe the data analysis. In Section 3, we present the results. The conclusions and the discussion of the source nature are given in Section 4.

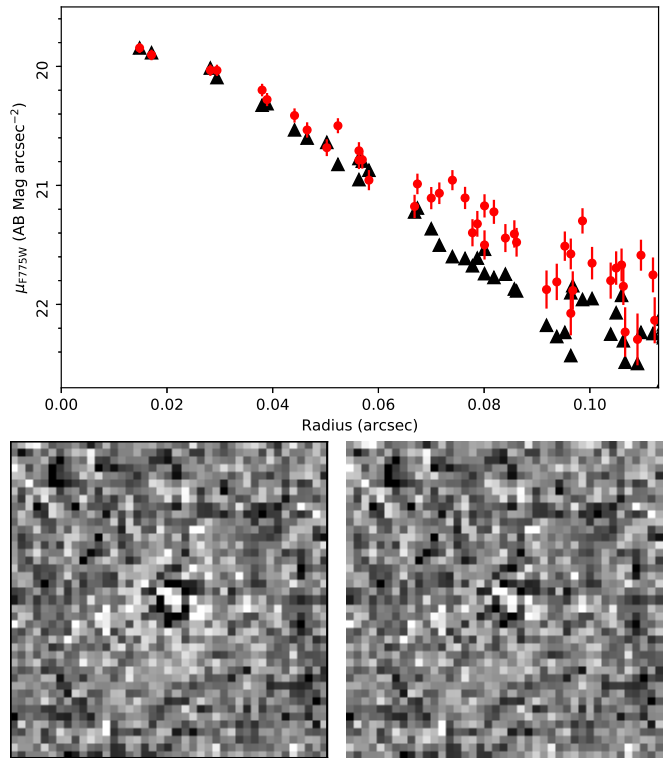


FIG. 2.— Top panel: the surface brightness of the star cluster in different pixels versus their distances to the derived center (red circle, 1σ error). The black triangles (errors are not shown but are negligible) are for the empirical PSF image (derived from nearby stars) with the center and the peak value forced to align with those of J2150–0551. Bottom panels: The two-dimensional residuals of the single Sérsic fits with index 1.0 (left) and 6.0 (right), using the GALFIT software.

2. DATA ANALYSIS

There are various multiwavelength observations of J2150–0551. In this Letter, we will focus on the new *XMM-Newton* and *HST* observations obtained in 2018, though we will also include some results of previous observations as obtained in Lin18. The new *XMM-Newton* observation (ObsID: 0823360101, X3 hereafter) was taken on 2018 May 24 in the imaging mode, with the exposure times of 49.3 ks, 57.8 ks, and 57.9 ks for the three European Photon Imaging Cameras (EPIC) pn, MOS1, and MOS2, respectively. We used SAS 16.0.0 and the calibration files of 2017 March as adopted in Lin18 for reprocessing the X-ray event files and follow-up analysis. There are no clear background flares seen in all cameras, and we used all data. We reprocessed the data and extracted the source light curve and spectra in the standard way, and we refer to Lin18 for details. Because the source was faint in X3, we adopt a circular source region of radius 20 arcsec.

The new *HST* observation was also carried out on 2018 May 24 under the program GO-15441, and it was to obtain an ACS/WFC image with the F775W filter, as adopted in the previous observation in 2003. It was composed of four exposures of 544 s each (2176 s in total). We produced the drizzled count image with the DrizzlePac software, with the pixel size set to be 0.03 arcsec. We performed a profile fit to the counterpart to J2150–0551 using two packages: one is GALFIT (Peng et al. 2010) and the other is ISHAPE (Larsen 1999). An empiri-

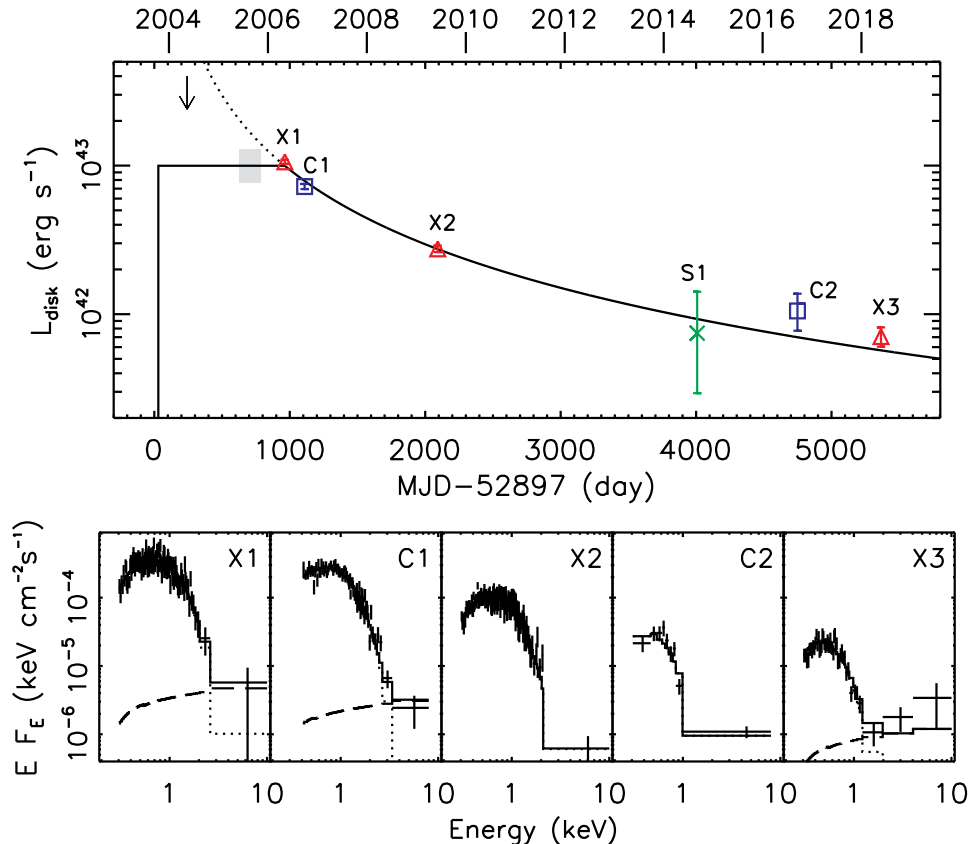


FIG. 3.— Top panel: the long-term bolometric disk luminosity curve with 90% errors from various pointed observations (*Chandra* blue squares, *XMM-Newton* red triangles, and *Swift* green cross). The downward arrow in 2004 marks the 3σ upper limit from an *XMM-Newton* slew observation and the gray shaded region marks the time interval when the optical flare was detected in 2005. The solid line is a simple TDE model, in which a very fast rise occurred one month after disruption and then the luminosity remained constant due to super-Eddington accretion effects (such as photon trapping), followed by a standard $t^{-5/3}$ decay. The dotted line neglects the super-Eddington accretion effects. Bottom panels: the standard thermal disk fits to the high-quality X-ray spectra at different epochs. A weak power-law was added to account for possible contamination from the nuclear emission of Gal1 in all fits except C2 (the nuclear source is spatially separated in this observation). For visual purposes, the spectra are rebinned to be above 2σ in each bin in the plot. For *XMM-Newton* observations, only pn spectra are shown. The plot is the same as Figure 2 in Lin18 except that we have added the new *XMM-Newton* observation X3 and have updated the TDE model in the upper panel.

cal point-spread function (PSF) was derived from four nearby stars, with an oversampling factor of ten.

3. RESULTS

3.1. Deep Optical Imaging

Figure 1 shows the new *HST* ACS F775W image around J2150–0551. The quality of the image around the source is significantly improved compared with the one obtained in 2003, due to twice the exposure length and better cosmic ray rejection (note the location of the source in the CCD gap in two previous exposures). We measured the magnitude of F775W = 24.08 ± 0.01 mag (AB, 1σ error) and 24.02 ± 0.02 mag from the 2018 and 2003 images, respectively, using an aperture of radius 0.3 arcsec (the background was estimated from four nearby circular regions of the same size). Therefore, we observed no clear optical variability between these two epochs. Because the 2003 image was taken before the outburst and thus represents the quiescence emission level (Lin18), the optical outburst, which was detected in 2005, must have subsided to below the detection level in 2018.

The counterpart seems marginally resolved in the 2018 image. This can be seen from the comparison of its radial profile with that of the PSF shown in the top panel in

Figure 2.

We first used GALFIT to fit the optical profile of the source in the new *HST* image with a single Sérsic function (convolved with the PSF). At the position of the source, there is star light from the host galaxy Gal1. Then there are also concerns about the size of the fitting region and how to model the background (sky plus the star light from Gal1). We first tried a fitting region of $1''.2 \times 1''.2$ centered around the source. The background was allowed to be variable and have a linear gradient. The profile seems symmetric, and the fit inferred the axis ratio to be consistent with 1.0. Therefore we fixed the value of this parameter at 1.0. We found that the fits preferred a large Sérsic index. The bottom panels of Figure 2 compare the fit residuals of index fixed at 1.0 (left) and those of index fixed at 6.0 (right). The fit with index 6.0 is reasonably acceptable (reduced χ^2 value of $\chi^2_\nu = 0.920$ for $\nu = 1675$ degrees of freedom) and is better than that of index 1.0, with the total χ^2 reduced by 94.0. Assuming a higher value of index would reduce the χ^2 value further but very slightly. The inferred half-light radius is not sensitive to the index value assumed and was inferred to be around 0.024–0.026 arcsec (i.e. 26–28 pc). The integrated magnitude is fainter for smaller in-

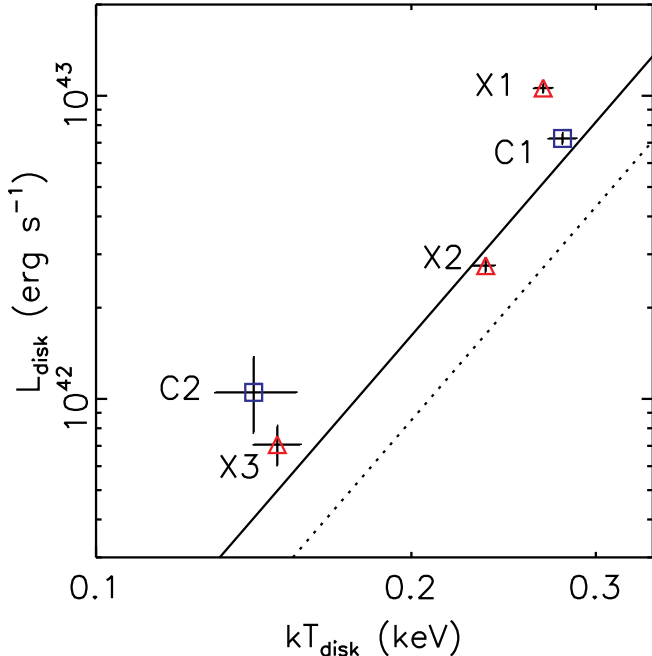


FIG. 4.— The disk luminosity versus the apparent maximum temperature, with 90% errors. The solid line plots the $L \propto T^4$ relation with the inner disk radius being the mean value of C1, X2, C2, and X3, weighted by the errors, while the dotted line plots the same relation but for ESO 243–49 HLX-1 (Servillat et al. 2011).

dex (F775W = 24.13 mag for index 1.0 and 23.92 mag for index 6.0). We note that the fits do not require a background gradient, which means that the fitting region used is not too large. The inferred background value from all fits is consistent with the median from an annulus of inner and outer radii of 0.5 arcsec and 0.7 arcsec, respectively.

There is no significant improvement to the fit using two Sérsic functions, reducing the χ^2 value by only 20, compared with the single Sérsic fit with index 6.0. The parameters could not be constrained well, and one possible good fit could be two Sérsic functions, with index 1.0 and 4.0 (fixed), effective radius 140 pc and 5 pc, and integrated magnitude F775W = 25.01 mag and 24.37 mag, respectively.

We also tested other popular models that are often used to fit star clusters. With a Moffat model of index 1.5, we obtained a reasonable fit ($\chi^2_\nu = 0.935$) with an effective radius of 27 pc. Using a King model, we obtained reasonable fits ($\chi^2_\nu \sim 0.92$) with large concentration values and effective radius ~ 23 pc. These fits suggest that although there are multiple models that can fit the optical counterpart to J2150–0551 well, the inferred effective radius is fairly consistent among different models.

We also used ISHAPE to carry out fits. We obtained consistent results with those with GALFIT. ISHAPE inferred the effective radius from various models to range between 26–32 pc.

3.2. X-ray follow-up

The X-ray spectrum of J2150–0551 from X3 is very soft, with most emission from low-energy photons below 1 keV (Figure 3). Therefore, the source should be still in the thermal state, and we fit the spectrum with an absorbed standard thermal disk model (*diskbb* in XSPEC)

as we did for previous observations (Lin18). A very weak powerlaw of a photon index fixed at 1.8 was included to account for contamination of the nuclear emission from Gal1, as was found in the high-resolution *Chandra* observation in 2016 (C2, Lin18). We inferred the disk apparent maximum temperature to be 0.149 ± 0.008 keV and the disk bolometric luminosity to be $7 \pm 1 \times 10^{41}$ erg s $^{-1}$ (errors are 90%). The luminosity is 30% lower than that from the previous *Chandra* observation C2, but such a decrease is not significant due to the large error bar of the *Chandra* observation (Figure 3). Lin18 constructed a simple TDE model to explain the luminosity evolution of the event. The updated model from the inclusion of the new additional observation X3 is shown in Figure 3 (solid line in the upper panel). The disruption time was inferred to be on 2003 September 15 (close to the time 2003 October 18 found in Lin18), with 1σ uncertainty of 35 days. The luminosity in X3 is close to that predicted in the simple TDE model (within 1.7σ). According to the model, the total energy radiated until X3 was 1.7×10^{51} ergs, and the total mass accreted into the black hole until X3 was $0.069(0.1/\eta) M_\odot$, where η is the rest mass to radiation energy conversion efficiency in the sub-Eddington accretion phase.

The updated disk luminosity versus disk apparent maximum temperature plot including X3 is shown in Figure 4. The new observation is consistent (to within 1.7σ) with the $L \propto T^4$ relation traced out by C1, X2, and C2. This strongly supports that the source was still in the thermal state in X3.

4. DISCUSSION AND CONCLUSIONS

The most significant result of our multiwavelength follow-up observations is the confirmation of the optical counterpart to J2150–0551 as an extended but very compact source, when the optical emission associated with the X-ray activity has subsided to below detection level. The extended nature of the counterpart firmly rules out the Galactic cooling neutron star explanation for the source, which is the reason why we did not test the neutron star atmosphere model on X3 as we did for previous X-ray spectra in Lin18. Therefore, J2150–0551 should have an extragalactic origin and can be associated with either Gal1 or a background galaxy. The chance probability for J2150–0551 to be within 11.6 arcsec from the center of a bright galaxy like Gal1 is very small, only 0.01% (Lin18). The optical counterpart to J2150–0551 has a circularly symmetric compact profile, unlike most background galaxies. The high disk temperature of the outburst is also hard to explain if it is in a distant background galaxy, as will be discussed below. Therefore, J2150–0551 is most likely associated with Gal1.

With a half-light radius of ~ 27 pc, an absolute *V*-band magnitude of -12.3 AB mag and a stellar mass of $\sim 10^7 M_\odot$, the counterpart could be a massive globular cluster or a UCD resulting from a minor merger (Norris et al. 2014). The latter explanation is more likely, given that the host galaxy Gal1 seems to be in an epoch of active minor mergers (see the presence of a possible nearby minor merger of Gal2 with Gal1, Figure 1). This compact system has a stellar mass around the limit above which stellar systems could only be explained as remnant nuclei of tidally disrupted galaxies, instead of true ancient star clusters (Norris et al. 2019).

The other main result that we obtained is the continuing decay of the source luminosity according to a simple TDE evolution model. The X-ray light curve spans 12 years. In addition, the X-ray spectrum remained super-soft, with good statistics confirming the disk luminosity evolution following the $L \propto T^4$ relation. This is a smoking-gun evidence for the thermal state of an accreting BH. Although the $L \propto T^4$ relation is commonly seen in BH X-ray binaries, such a relation was only obtained in a few cases for accreting massive BHs, especially TDEs associated with nuclear SMBHs. Because the disk temperature depends on the BH mass as $M_{\text{BH}}^{-1/4}$ for a given Eddington ratio, it is expected that IMBHs have higher disk temperatures than SMBHs. This explains why the IMBH candidates J2150–0551 and ESO 243–49 HLX-1 (Servillat et al. 2011; Godet et al. 2012) have disk temperatures reaching ~ 0.25 keV, much higher than observed in SMBH TDEs that also exhibited $L \propto T^4$ ($\lesssim 0.1$

keV; Lin et al. 2011; Miniutti et al. 2019).

Acknowledgments: This work is supported by the National Aeronautics and Space Administration XMM-Newton GO program grant 80NSSC19K0873, by National Aeronautics and Space Administration through grant number HST-GO-15441.001-A from the Space Telescope Science Institute, which is operated by AURA, Inc., under NASA contract NAS 5-26555, and by the National Aeronautics and Space Administration ADAP grant NNX17AJ57G. JS acknowledges support from the Packard Foundation. AJR was supported as a Research Corporation for Science Advancement Cottrell Scholar. NW, OG and DB acknowledge CNES for financial support to the XMM-Newton Survey Science Center activities.

REFERENCES

- Abbott, B. P., Abbott, R., Abbott, T. D., et al. 2016, *Physical Review Letters*, 116, 061102
- Baldassare, V. F., Reines, A. E., Gallo, E., & Greene, J. E. 2015, *ApJ*, 809, L14
- Baumgardt, H., He, C., Sweet, S. M., et al. 2019, *MNRAS*, 488, 5340
- Chen, J.-H. & Shen, R.-F. 2018, *ApJ*, 867, 20
- Chilingarian, I. V., Katkov, I. Y., Zolotukhin, I. Y., et al. 2018, *ApJ*, 863, 1
- Dong, X., Wang, T., Yuan, W., et al. 2007, *ApJ*, 657, 700
- Event Horizon Telescope Collaboration, Akiyama, K., Alberdi, A., et al. 2019, *ApJ*, 875, L1
- Farrell, S. A., Webb, N. A., Barret, D., Godet, O., & Rodrigues, J. M. 2009, *Nature*, 460, 73
- Gillessen, S., Eisenhauer, F., Trippe, S., et al. 2009, *ApJ*, 692, 1075
- Godet, O., Plazolles, B., Kawaguchi, T., et al. 2012, *ApJ*, 752, 34
- Gravity Collaboration, Abuter, R., Amorim, A., et al. 2018, *A&A*, 618, L10
- Greene, J. E., Strader, J., & Ho, L. C. 2019, arXiv:1911.09678
- Irwin, J. A., Brink, T. G., Bregman, J. N., & Roberts, T. P. 2010, *ApJ*, 712, L1
- Israel, G. L., Belfiore, A., Stella, L., et al. 2017, *Science*, 355, 817
- Kızıltan, B., Baumgardt, H., & Loeb, A. 2017, *Nature*, 542, 203
- Komossa, S. 2015, *JHEA*, 7, 148
- Kormendy, J. & Richstone, D. 1995, *ARA&A*, 33, 581
- Larsen, S. S. 1999, *A&AS*, 139, 393
- Lin, D., Carrasco, E. R., Grupe, D., et al. 2011, *ApJ*, 738, 52
- Lin, D., Carrasco, E. R., Webb, N. A., et al. 2016, *ApJ*, 821, 25
- Lin, D., Strader, J., Carrasco, E. R., et al. 2018, *Nature Astronomy*, 2, 656
- Mann, C. R., Richer, H., Heyl, J., et al. 2019, *ApJ*, 875, 1
- Miniutti, G., Saxton, R. D., Giustini, M., et al. 2019, *Nature*, 573, 381
- Norris, M. A., Kannappan, S. J., Forbes, D. A., et al. 2014, *MNRAS*, 443, 1151
- Norris, M. A., van de Ven, G., Kannappan, S. J., Schinnerer, E., & Leaman, R. 2019, *MNRAS*, 488, 5400
- Noyola, E., Gebhardt, K., & Bergmann, M. 2008, *ApJ*, 676, 1008
- Peng, C. Y., Ho, L. C., Impey, C. D., & Rix, H.-W. 2010, *AJ*, 139, 2097
- Perera, B. B. P., Stappers, B. W., Lyne, A. G., et al. 2017, *MNRAS*, 468, 2114
- Remillard, R. A. & McClintock, J. E. 2006, *ARA&A*, 44, 49
- Servillat, M., Farrell, S. A., Lin, D., et al. 2011, *ApJ*, 743, 6
- Sutton, A. D., Roberts, T. P., Gladstone, J. C., & Walton, D. J. 2015, *MNRAS*, 450, 787
- Webb, N., Cseh, D., Lenc, E., et al. 2012, *Science*, 337, 554